Available online at www.sciencedirect.com
SCIENCE DIRECT
Carbohydrate Research 341 (2006) 2098–2107
Carbohydrate RESEARCH

Electrospun nano-fibre mats with antibacterial properties from quaternised chitosan and poly(vinyl alcohol)

Milena Ignatova,[a] Kirilka Starbova,[b] Nadya Markova,[c] Nevena Manolova[a] and Iliya Rashkov[a,*]

[a]*Laboratory of Bioactive Polymers, Institute of Polymers, Bulgarian Academy of Sciences, 1113 Sofia, Bulgaria*
[b]*Central Laboratory of Photoprocesses, Bulgarian Academy of Sciences, 1113 Sofia, Bulgaria*
[c]*Institute of Microbiology, Bulgarian Academy of Sciences, 1113 Sofia, Bulgaria*

Received 2 February 2006; received in revised form 19 April 2006; accepted 8 May 2006
Available online 5 June 2006

Abstract—Nano-fibres containing quaternised chitosan (QCh) have been successfully prepared by electrospinning of QCh solutions mixed with poly(vinyl alcohol) (PVA). The average fibre diameter is in the range of 60–200 nm. UV irradiation of the composite electrospun nano-fibrous mats containing triethylene glycol diacrylate as cross-linking agent has resulted in stabilising of the nano-fibres against disintegration in water or water vapours. Microbiological screening has demonstrated the antibacterial activity of the photo-cross-linked electrospun mats against *Staphylococcus aureus* and *Escherichia coli*. The obtained nano-fibrous electrospun mats are promising for wound-healing applications.

Keywords: Electrospinning; Chitosan derivatives; Photo-mediated cross-linking; Water-stable nano-fibrous mats; Antibacterial activity

1. Introduction

Polymers having intrinsic bacteriostatic and/or bactericidal activity are of interest as wound-dressing materials. Polysaccharides are considered as promising for wound-healing and wound-dressing applications.[1–4] The natural polysaccharide chitosan is reported to possess advantageous biological properties, for example, haemostatic activity, non-toxicity, biodegradability, intrinsic antibacterial properties and the ability to affect macrophage function, which contributes to faster wound healing.[1–3] Quaternised chitosan (QCh) derivatives have shown higher activity against bacteria, broader spectrum of activity and higher killing rate as compared to those of chitosan[5–7] and thus are potential candidates for wound-dressing applications. Electrospinning is an attractive approach to the fabrication of fibrous materials for variety of applications, including wound dressings, tissue scaffolds, vascular grafts, drug delivery, sensors and filter.[8–12] Electrospun mats from ultrafine polymer fibres are drawing a great attention because of their unique properties such as high surface-to-volume ratio, high porosity and diameters in the nano-scale. Nano-fibres have been successfully electrospun from water-soluble non-ionogenic polymers such as polyoxyethylene[13] and poly(vinyl alcohol) (PVA).[14,15] PVA is of particular interest for wound dressings since it is highly hydrophilic, has an inherent fibre- and film-forming ability, and can be easily cross-linked. Cross-linking of electrospun PVA mat in the solid state has been reported.[14,16,17] Recently, it has been shown that the preparation of nano-fibres of polyelectrolytes by electrospinning of their aqueous solutions is feasible only in the presence of a second polymer. Nano-fibrous chitosan-containing hybrid mats have been electrospun from mixed solutions of chitosan and polyoxyethylene,[18,19] of chitosan and silk fibroin,[20] of chitosan and PVA,[21,22] of *N*-carboxyethylchitosan and polyacrylamide.[23] Nano-fibres from

* Corresponding author. Tel.: +359 29793468; fax: +359 28700309; e-mail: rashkov@polymer.bas.bg

0008-6215/$ - see front matter © 2006 Elsevier Ltd. All rights reserved.
doi:10.1016/j.carres.2006.05.006

homopolymer of 2-acryloylamido-2-methylpropanesulfonic acid (PAMPS) and from its copolymers with acrylic acid (P(AMPS-co-AA)) have been obtained by electrospinning of mixed PAMPS/PVA or P(AMPS-co-AA)/PVA solutions.[23] Previously, we have shown that after immobilisation of model drugs (8-hydroxyquinoline derivatives) in chitosan- or *N*-carboxyethylchitosan-containing nano-fibres, they acquire antimicrobial and antimycotic activity.[20,23]

The first goal of the present work is to study the preparation of quaternised chitosan-containing nano-fibres by electrospinning of mixed QCh/PVA aqueous solutions. Further, stabilisation of the nano-fibres with respect to aqueous medium has been achieved using photo-mediated cross-linking. The antibacterial properties of photo-cross-linked electrospun QCh/PVA mats are also studied.

2. Experimental

2.1. Materials

n-Butyraldehyde, $NaBH_4$, CH_3I, NaI, poly(vinyl alcohol) (PVA) ($M_W = 4.9 \times 10^4$, degree of hydrolysis 86–89%), 2,2-dimethoxy-2-phenylacetophenone (DMPA) and ammonium peroxydisulfate were purchased from Fluka. The products were with analytical grade of purity. Triethylene glycol diacrylate (TEGDA) (Aldrich) was purified by column chromatography (eluent heptane/chloroform/ethanol = 8:50:5, Silicagel 60). Prior to use, *N*-methyl-2-pyrrolidone (NMP) (Fluka) was freshly distilled under reduced pressure. Chitosan with molecular weight of 400,000 g/mol (Aldrich) with 80% degree of deacetylation was used.

2.2. Preparation and characterisation of *N*-butyl-*N*,*N*-dimethyl chitosan iodide

N-Butyl-*N*,*N*-dimethyl chitosan iodide (QCh) was prepared according to two-step procedure described by Kim et al.[5] Briefly, to 1% w/v chitosan (7 g) solution in 1% aqueous acetic acid, 32.8 g (41 mL) of *n*-butyraldehyde (11-fold molar excess of aldehyde to glucosamine unit) was added. After 1 h of stirring at room temperature, the pH of the solution was adjusted to 4.5 and 10% aqueous solution of $NaBH_4$ (1.5-fold molar excess to added *n*-butyraldehyde) was added. The reaction mixture was stirred for 2.30 h. *N*-Butyl chitosan derivative was collected as precipitate by adjusting the pH of the solution to 10. The precipitate was washed to neutrality by distilled water. The product was purified from unreacted aldehyde and inorganic products by Soxhlet-extraction with ethanol and diethylether for 4 days. The obtained *N*-butyl chitosan was filtered out and vacuum dried at 40 °C for 2 days. Yield—5.3 g (52%).

N-Butyl chitosan (4.7 g) was dispersed in 250 mL of NMP for 12 h at room temperature. Thirty milliliters of 1.4 M aqueous solution of NaOH and 19.5 mL CH_3I (2- and 15-fold molar excess to amine group of chitosan, respectively) were added. The reaction was carried out for 12 h at 50 °C. The product was purified by twice precipitation with acetone and vacuum dried at 40 °C. Yield—8.2 g (94%).

Fourier transform infrared (FT-IR) spectra of films (QCh) and mats (QCh/PVA and PVA) were recorded on a Bruker Vector 22 Infrared Spectrometer at room temperature on KBr pellets. NMR spectra were taken on a Bruker spectrometer (400.13 MHz for ^1H and 125.67 MHz for ^{13}C) at 333 K in D_2O, using TMS for reference. The degree of quaternisation of QCh was determined by the ^1H NMR data and by potentiometric titration of the iodide form with aqueous silver nitrate, using working silver electrode and reference calomel electrode.

IR: *N*-butyl chitosan (on KBr pellets): 3424 (N–H stretching vibration), 2958, 2925 and 2872 (C–H stretching vibration from *N*-butyl residue and from polysaccharide structure), 1664 (amide I), 1560 (amide II from polysaccharide structure), 1466 (antisymmetric C–H deformation of the *N*-butyl group), 1382 (symmetric C–H deformation of the *N*-butyl group) and 1069 cm^{-1} (C–O–C stretching vibration).

IR: *N*-butyl-*N*,*N*-dimethyl chitosan iodide (film): 3416 (N–H stretching vibration), 2961, 2936, 2876 (C–H stretching vibration from *N*-butyl- and *N*,*N*-dimethyl residues and from polysaccharide structure), 1651 (amide I), 1548 (amide II), 1470 (antisymmetric C–H deformation of the *N*-butyl-*N*,*N*-dimethyl group), 1379 (symmetric C–H deformation) and 1063 cm^{-1} (C–O–C stretching vibration).

^1H NMR (D_2O): δ 0.97 (CH_3– from *N*-butyl group), 1.4 (CH_3–CH_2–$(CH_2)_2$–), 1.8 (CH_3–CH_2–CH_2–CH_2–), 2.1 (–NHCOCH_3), 3.1 (–CH_2–N^+–$(CH_3)_2I^-$), 3.4 (CH_3–O-6), 3.5 (CH_3–O-3), 3.8 (H-2 and H-6), 4.0 (H-3), 4.2 (H-5), 4.3 (H-4) and 5.2 ppm (H-1).

^{13}C NMR (D_2O): δ 13.5 (CH_3–CH_2–$(CH_2)_2$–), 19.8 (CH_3–CH_2–$(CH_2)_2$–), 27.2 (CH_3–CH_2–CH_2–CH_2–), 54.8 (($CH_3)_2$–N^+–), 57.7 (CH_3–$(CH_2)_2$–CH_2–), 61.5 (C-6), 69.1 (C-4), 75.4 (C-5), 77.7 (C-3), 77.2 (C-2) and 95.8–101.7 ppm (C-1).

The degree of methylation of –OH functions is determined from the ratios between the integrated areas of the signals of CH_3–O at 3.5 and 3.4 ppm, for OH at C-3 and C-6 position, respectively, and the integrated area of the H-1 signals. The degree of methylation of H-3 and H-6 was 13% and 88%, respectively. The quaternisation degree is calculated from the ratio between the integrated areas of the signal at 3.1 ppm for –CH_2–N^+–$(CH_3)_2I^-$ and that of the H-1 signals.

2.3. Preparation of the spinning solutions QCh/PVA and electrospinning

The spinning solutions QCh/PVA were prepared by mixing 8% aqueous PVA solution with 8% aqueous solutions of QCh at weight ratios of QCh:PVA = 1:4, 2:3, 1:1, 3:2 and 4:1. The total polymer concentration in the mixed solutions was 8 wt %.

The dynamic viscosity of the spinning solutions was measured using a Brookfield LVT viscometer equipped with a small-sample thermostated adapter, spindle and chamber SC4-18/13R, at 25 ± 0.1 °C. The electrical resistance of the spinning solutions was measured in a specially designed electrolytic cell equipped with rectangular sheet platinum electrodes having a surface area of 0.006 cm^2 and disposed at a distance of 2.0 cm. During the measurements short electric pulses with opposite direction were applied to Pt electrodes in order to avoid accumulation of ionic charge and polarisation effects in the vicinity of electrode surface. This allowed solution resistance in the range 20–2000 kΩ to be measured with an accuracy of ±3%. The conductivity of the spinning solutions (σ) was calculated from the following Eq. 1:

$$\sigma = \frac{1}{\rho} = \frac{L}{R \cdot S} \tag{1}$$

where ρ is the specific resistance of the solution, R the electrical resistance of the solution, L the distance between the electrodes and S the surface area of electrode.

The mixed solutions (3 mL) were placed into a 3 mL plastic syringe equipped with a nozzle ($d = 0.1$ mm). An electrode connected with a high voltage supply capable of generating positive DC voltages (10–40 kV) was immersed in the syringe. A grounded copper plate was used as a collector. The collected nano-fibres were placed in a vacuum oven overnight at 40 °C to fully eliminate solvent residuals.

The solution entanglement number $(n_e)_{soln}$ was estimated from Eq. 2:[24]

$$(n_e)_{soln} = \frac{M_w}{(M_e)_{soln}} = \frac{(\phi_p M_w)}{M_e} \tag{2}$$

where M_w is weight-average molar mass of polymer, $(M_e)_{soln}$—entanglement molecular weight in solution, M_e—entanglement molecular weight in melt, ϕ_p—polymer volume fraction.

2.4. Photo-mediated cross-linking of electrospun nano-fibres and films

The solutions for the preparation of cross-linked nano-fibres and of solution-cast films were prepared as follows. TEGDA (10.7%), DMPA (1%) in DMSO and ammonium peroxydisulfate (1%) (all in weight percent to total polymer content) were added to the solution QCh/PVA at weight ratio of QCh:PVA = 2:3. The total polymer concentration in the mixed solutions was 10 wt % (H_2O/DMSO = 92:8 w/w). Films were cast from the solutions into Petri dishes and left to dry at 40 °C in the dark before UV irradiation. In order to perform photo-cross-linking, the electrospun mats or the films were irradiated with a UV lamp HBO (Germany) (365 nm, 200 W). The distance between the UV lamp and the electrospun mat was maintained at 50 cm. The UV irradiation was performed at room temperature for 10 h.

To determine the stability of photo-cross-linked electrospun mats against water, they were immersed in distilled water for 1 h. The stability of the photo-cross-linked nano-fibres against water vapour was studied by placing the disks covered with non-woven mats in a desiccator at 100% air humidity at 23 °C for 1 h. The treated samples were dried at 45 °C to constant weight and the nano-fibre morphology was examined by SEM microscopy.

The swelling degree (α) of the photo-cross-linked electrospun QCh/PVA mats was determined gravimetrically and was calculated from the following Eq. 3:

$$\alpha\ \% = \frac{\text{weight of swollen mat} - \text{weight of dry mat}}{\text{weight of dry mat}} \times 100 \tag{3}$$

The time duration for swelling was 24 h.

2.5. Characterisation of the electrospun QCh/PVA mats

The nano-fibres collected onto aluminium plates were vacuum-covered with carbon (*Jeol JFC-1200 fine coater*) and examined in a scanning electron microscope *Jeol JSM-5510*. The average fibre diameter, the standard deviation, the width and length of the defects and the average distance between the defects along a fibre were evaluated using *Image J* software program by measuring 30 fibres from each SEM image.

2.6. Antibacterial assessment

The minimum inhibitory concentration (MIC) of QCh was determined for *Escherichia coli* 3588, *Staphylococcus aureus* 749, respectively. A preculture of the different bacteria was grown overnight in meat-peptone broth at 37 °C under orbital agitation. The culture was diluted with fresh media to 1.2×10^6 cells/mL (determined optically using a standard). The tested polymer was dissolved in distilled water at an initial concentration of 0.033 g/mL. Additional solutions were prepared by the serial dilution method and incubated at 37 °C for 24 h.

The antibacterial activity of photo-cross-linked electrospun QCh/PVA mat, of photo-cross-linked QCh/PVA film and of PVA mat against the Gram-positive

bacteria *S. aureus* and Gram-negative *E. coli* was assessed by a viable cell-counting method.[25] Upon appropriate dilution with sterilised 0.9% saline solution, a culture of about 10^4 cell/mL was prepared and used for antibacterial testing. Mats electrospun onto aluminium collectors were put into different tubes. All electrospun mats were sterilised by UV irradiation and exposed to the bacteria (*S. aureus* or *E. coli*) cell suspension (5 mL containing about 10^4 cells/mL). At a specified time, 1 mL of bacteria culture was added to 9 mL of sterilised 0.9% saline solution, and several decimal dilutions were repeated. The surviving bacteria were counted by the spread-plate method. At various exposure times, 0.1-mL portions were removed and quickly spread on the nutrient agar. After inoculation, the plates were incubated at 37 °C for 24 h, and the colonies were counted. Counting was triplicated for each experiment. The reduction of bacteria was calculated according to the following equation: Reduction $(\%) = (B - A)/B \times 100$, where A and B are the surviving cells (colony forming unit mL^{-1}) for the plates containing test samples and the control, respectively, after 30, 60, 90 and 120 min contact time.

3. Results and discussion

3.1. Electrospinning of QCh/PVA mixed solutions

Quaternised chitosan (QCh, Scheme 1) was prepared as described in the literature.[5] The quaternisation degree determined by ^{1}H NMR was 82%. The data from potentiometric titration are close to that of the NMR data (80%). The degree of methylation of the –OH group on C-3 and C-6 was 13% and 88%, respectively, as determined by ^{1}H NMR spectroscopy.

Our preliminary attempts for electrospinning of solutions of QCh in distilled water over a broad concentration range failed to obtain ultrafine fibres. In this case, formation of 'tailed' micro- and nano-particles was observed. This might be due to the repulsive force between ionogenic groups within polymer backbone that impede the formation of continuous nano-fibres during electrospinning process. Previously, it was found that the presence of a non-ionogenic polymer with a flexible chain in the spinning solution facilitates the nano-fibre formation from ionogenic polymers.[18–23] In the present study, we have selected PVA as a suitable non-ionogenic partner for the preparation of QCh-containing nano-fibres.

IR spectroscopy was applied to characterise QCh/PVA mixed nano-fibres (Fig. 1). The IR spectra of the electrospun QCH/PVA mats showed the absorption characteristics of both the QCh and PVA constituents. Bands at 1655 and 1548 cm^{-1}, respectively, for amide I and amide II from polysaccharide structure of QCh were observed. By increasing the weight ratio of QCh to PVA from 2:4 to 1:1, a shoulder at 1470 cm^{-1} assignable to the stretching vibration of $–CH_3$ and $–CH_2$ groups next to the quaternised ammonium group appeared. The intensity ratio of the amide I band (1653 cm^{-1}) and the band at 1732 cm^{-1} (characteristic for C=O stretching vibration from PVA) decreased on increasing the weight ratio of QCh to PVA from 2:4 to 1:1.

At a molar mass of PVA 49,000 g/mol, on decreasing the total solution QCh/PVA concentration from 13 to 8 wt %, the average fibre diameter decreased and the shape of the fibres changed from flat to cylindrical one (Fig. 2). The same tendency was observed in the case of electrospinning of PVA.[26] The average diameters of fibres electrospun at a weight ratio of QCh:PVA = 1:4 at applied field strength (AFS) of 2 kV/cm were 600 and 145 nm for total polymer concentration 13 and 8 wt %, respectively. Thus, for electrospinning of QCh/PVA mixed solutions the found optimal conditions were the following: total polymer concentration 8 wt % and AFS values in the range from 1.5 to 3.5 kV/cm.

The morphology of electrospun nano-fibres (presence or absence of defects, shape of the fibres and the defects) and their average diameters are strongly influenced by the composition of the spinning solution.[15,18,23] The viscosity of 8 wt % aqueous solution of PVA was 197 cP and that of QCh was 181 cP. The dynamic viscosity of the solutions of QCh and PVA mixed at weight ratios of QCh:PVA = 1:4, 2:3, 1:1, 3:2 and 4:1 was 217, 213, 194, 190 and 187 cP, respectively. As seen from the results, regardless of the insignificant difference in the viscosity of the solutions of PVA, QCh or mixed QCh/PVA solutions, fibres with different morphology were formed on varying the ratios QCh/PVA. The increase in

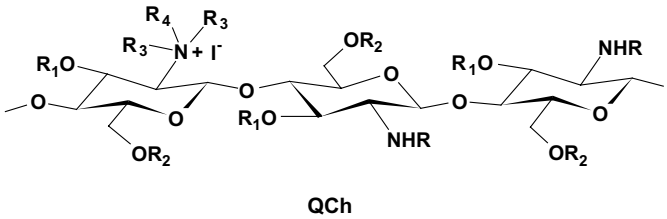

QCh

Scheme 1. Quaternised chitosan (QCh) chain sequence. R = H (14%), C(O)CH_3 (20%), R_1 = H (87%), CH_3 (13%), R_2 = H (12%), CH_3 (88%), $R_3 = CH_3$ (66%), $R_4 = C_4H_9$ (66%).

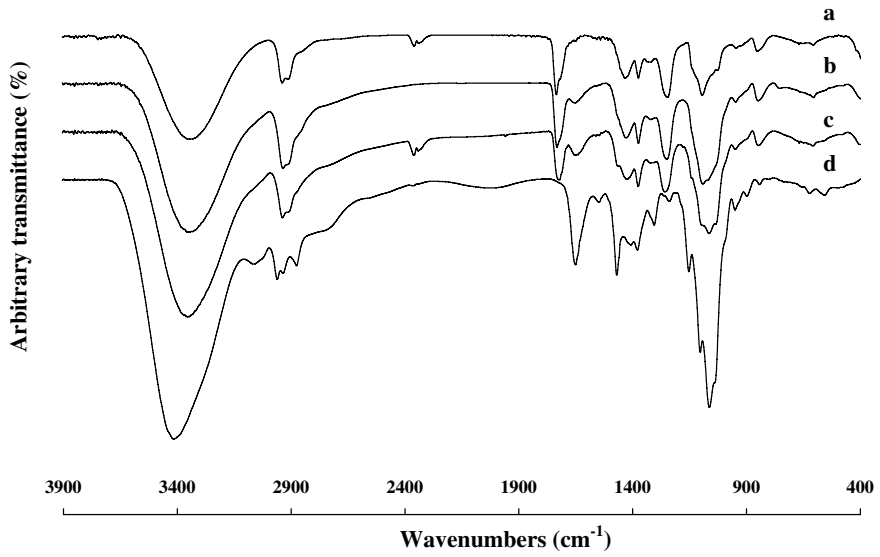

Figure 1. FT-IR spectra of (a) electrospun PVA mat, (b) electrospun QCh/PVA mat (weight ratio QCh:PVA = 2:4), (c) electrospun QCh/PVA mat (weight ratio QCh:PVA = 1:1) and (d) QCh film.

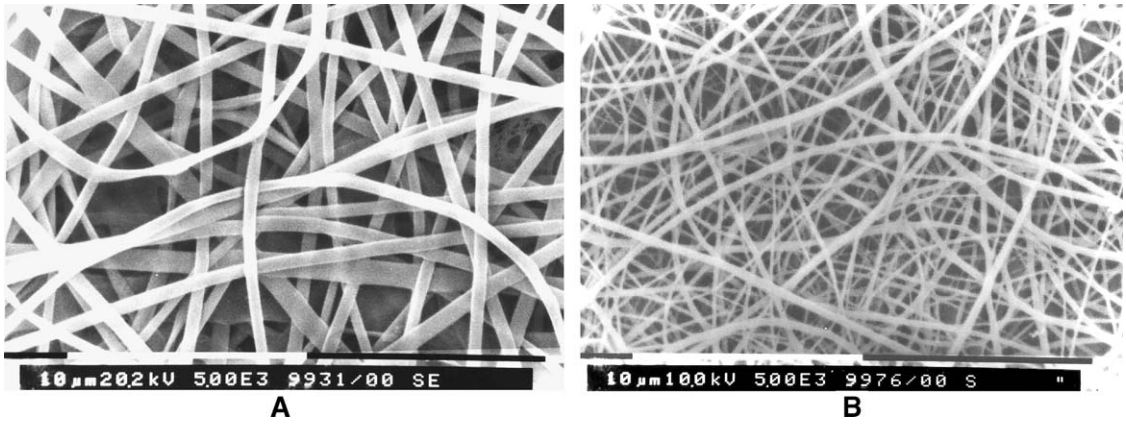

Figure 2. SEM micrographs of nano-fibres prepared from QCh/PVA mixed solutions; QCh:PVA = 1:4 (w/w). Total polymer concentration: 13 wt % (A), 8 wt % (B). AFS 2.0 kV/cm.

the content of ionogenic polymer QCh led to a decrease in the average diameter of the nano-fibres and to an increase in the amount of spindle-like defects. This change in the morphology might be explained with the increase in the charge density and with increase of the solution conductivity (Table 1) on increasing the content of the polyelectrolyte QCh. Cylindrically shaped continuous nano-fibres without defects were formed by electrospinning of solutions with high PVA content (QCh:PVA = 1:4) at AFS from 1.5 to 2.7 kV/cm (Fig. 3 and Table 2). At an AFS value of 3.5 kV/cm, a small number of spindle-like defects of size 480 × 3400 nm were formed due to jet instability at high AFS. On increasing the polyelectrolyte content at constant AFS value (1.5 kV/cm), the fibre diameters decreased—for example, from 200 to 70 nm in the case of QCh/PVA = 1:4 and 3:2, respectively. An increase in the amount of spindle-like defects and narrowing of the fibre diameter distribution were also observed (Fig. 3). These results are in agreement with the results obtained previously.[18,23] The increase in QCh content at constant AFS value 2.0 kV/cm led to an increase in the width/length ratio of the spindle-like defects—for example, from 0.23 to 0.40 in the case of QCh:PVA = 2:3 and 3:2, respectively. The average distance between two neighbouring defects

Table 1. Conductivity (σ) of the mixed aqueous solutions at different weight ratios of QCh/PVA

QCh/PVA[a] (w/w)	1:4	2:3	1:1	3:2	4:1
σ (mS/cm)	2.3	3.2	3.7	4.1	6.0

Total polymer concentration 8 wt %.

[a] σ (mS/cm) of 8 wt % aqueous solutions of PVA and of QCh were 0.96 and 7.20, respectively.

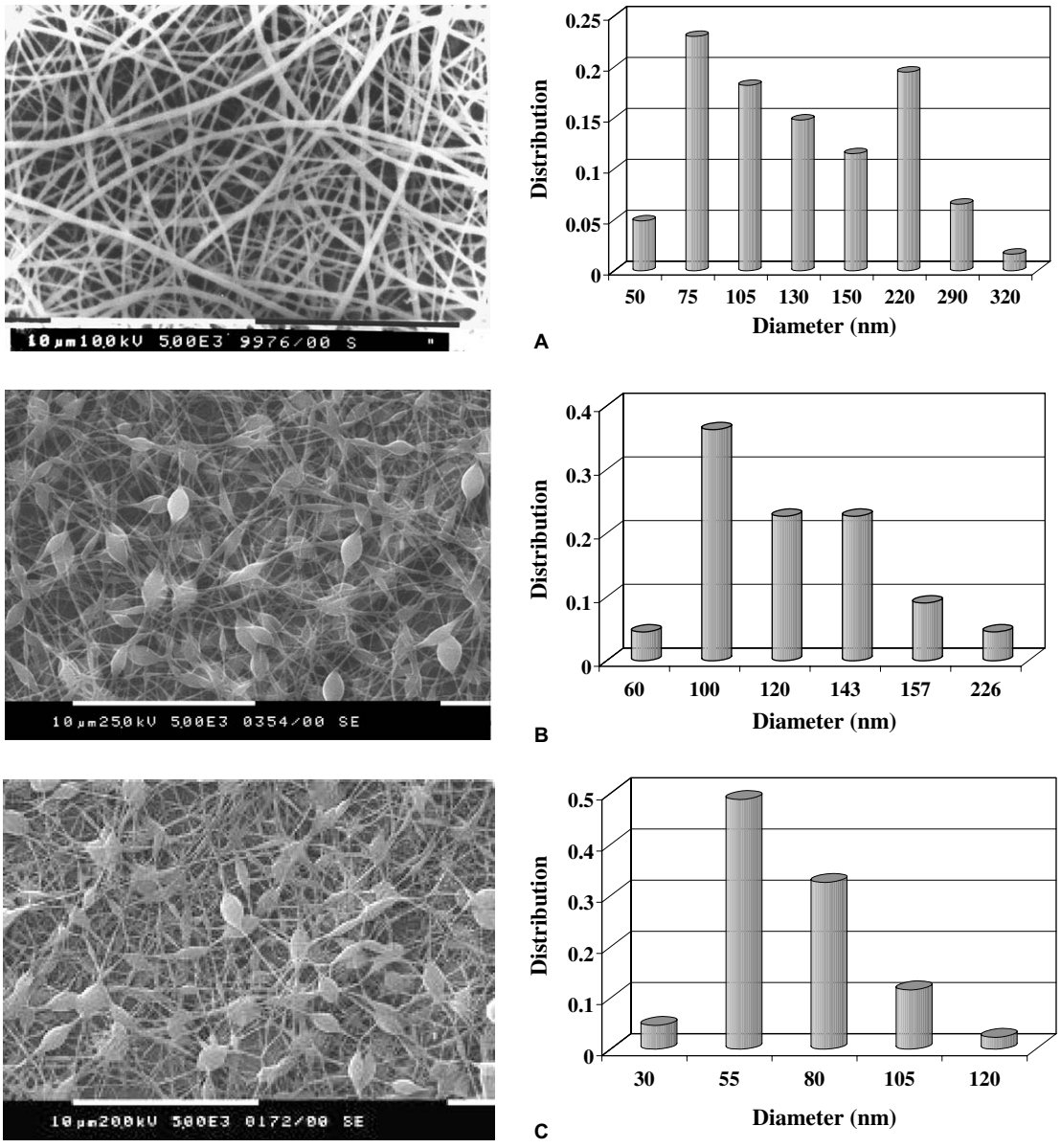

Figure 3. SEM micrographs and diameter distribution of the nano-fibres prepared from QCh/PVA mixed solutions. Weight ratio QCh:PVA = 1:4 (A); 2:3 (B) and 1:1 (C). Total polymer concentration 8 wt %, AFS 2.0 kV/cm.

along a fibre decreased from 3400 to 1615 nm in the case of QCh/PVA = 2:3 and 3:2, respectively (at AFS = 2.0 kV/cm). On further increase of the content of quaternised chitosan derivative (QCh:PVA = 4:1), continuous nano-fibres did not form and only non-connected with the fibres 'tailed' beads were observed (Fig. 4B).

The polymer concentration necessary for the formation of nano-fibres without defects can be estimated using the semi-empirical methodology proposed by Shenoy et al.,[24,27] taking into account the solution entanglement number—$(n_e)_{soln}$. According to these authors, fibre formation is initiated at $(n_e)_{soln} \sim 2$, while the critical polymer concentration necessary for continuous fibre formation (fibres without defects) corresponds to $(n_e)_{soln} = 3.5$. The $(n_e)_{soln}$ values of PVA in the spinning solutions with different weight ratios of QCh and PVA were estimated taking into account the concentration of PVA in the mixed solutions (Table 2). Since the entanglement molecular weight in melt for QCh (M_{eQCh}) was not possible to be estimated, the $(n_e)_{soln}$ value for aqueous solution of QCh was impossible to be determined. The results showed that nano-fibres without defects were formed by electrospinning of mixed solutions at weight ratio of QCh:PVA = 1:4. In this case, the $(n_e)_{soln}$ value for PVA was 0.7—a value significantly lower than 3.5, estimated by the entanglement analysis. Spindle-like defects along the fibres were observed at weight ratios of QCh:PVA (w/w) = 2:3, 1:1 and 3:2, where $(n_e)_{soln}$ was 0.5, 0.4 and 0.3, respectively. Similar effect has also been observed by other authors in the case of

Table 2. Composition of the mixed solution QCh/PVA, applied field strength (AFS), average fibre diameter ($\bar{d}$), standard deviation (SD), width (W) and length (L) of the defects and solution entanglement number $(n_e)_{soln}$

QCh/PVA (w/w)	$(n_e)_{soln}$ [a]	AFS (kV/cm)	$\bar{d}$ (nm)	SD	W/L (nm)
1:4	0.7	1.5	200	88	No defects
		2.0	145	72	No defects
		2.7	135	63	No defects
		3.5	125	47	480/3400
2:3	0.5	1.5	130	78	370/2100
		2.0	130	34	610/2700
		2.7	130	55	600/2500
		3.5	120	77	440/3300
1:1	0.4	1.5	75	28	950/1800
		2.0	70	20	510/1900
		2.7	65	28	560/1500
		3.5	60	12	470/1500
3:2	0.3	1.5	70	22	550/1000
		2.0	70	22	580/1440
		2.7	60	28	550/1800
		3.5	60	17	540/1300

Total polymer concentration 8 wt %.
[a] $(n_e)_{soln}$ value of PVA was estimated by using Eq. 1, taking into account the concentration of PVA in the mixed solutions.

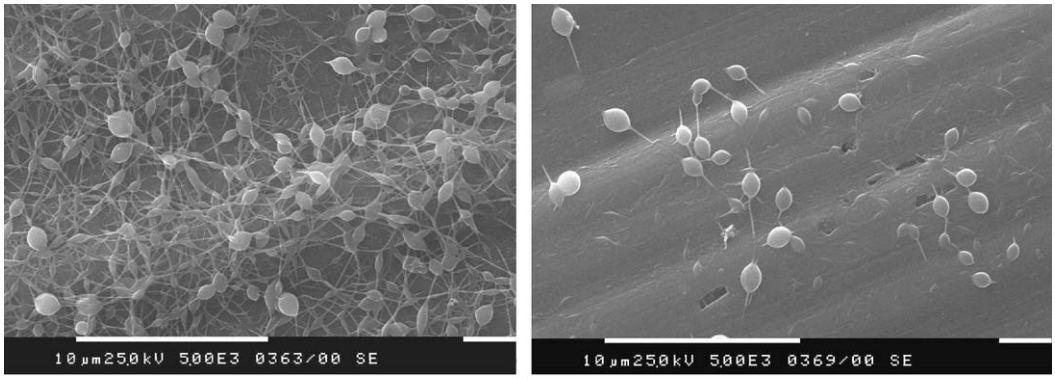

Figure 4. SEM micrographs of electrospun QCh/PVA mixtures at weight ratios QCh:PVA = 3:2 (A); and 4:1 (B). Total polymer concentration 8 wt %, AFS 2.0 kV/cm.

electrospinning of aqueous solutions of PVA [17,26,27] and has been explained by Shenoy et al.[27] with the ability of PVA solutions to undergo physical gelation because of inter- and intramolecular hydrogen bonding. The significantly lower $(n_e)_{soln}$ value necessary for the preparation of nano-fibres without defects in the case of electrospinning of QCh/PVA mixed solutions might be explained with the presence of the second polymer (QCh), which is also capable to participate in hydrogen bonding.

It has been reported that AFS also has an effect on the nano-fibre morphology and the average fibre diameter.[15,18,23] In order to follow the effect of AFS, a series of experiments for electrospinning of QCh/PVA mixed solutions were carried out at constant weight ratio between the polymer partners and varying the AFS from 1.5 to 3.5 kV/cm (Table 2). It was found that the average diameters of nano-fibres slightly decreased on increasing the AFS value. This finding is in accordance with data of other authors.[15,28,29] The decrease of the fibre diameter by increasing the electric field, while maintaining the distance between the spinneret and the collector, is attributed to the increase of the force, which pulls and stretches the polymer jet. At a higher AFS value, the number of spindle-like defects increased. The increase in AFS had insignificant effect on the average sizes of defects along the fibres (Table 2).

3.2. Photo-mediated cross-linking of the electrospun QCh/PVA nano-fibres

When the QCh/PVA nano-fibrous mats were immersed in water, they readily dissolved. The possibilities for application of the electrospun mats might be significantly enlarged if they are made stable in aqueous

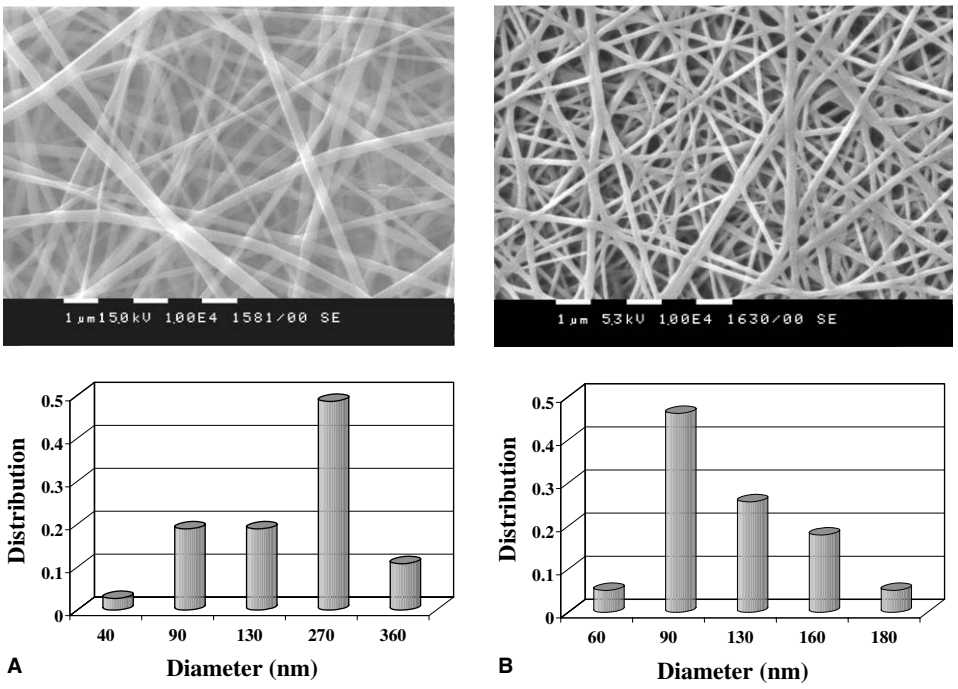

Figure 5. SEM-micrographs and average diameter distribution of the nano-fibres prepared from QCh:PVA solutions without (A), and in the presence of 1 wt % DMPA, 1 wt % ammonium peroxydisulfate and 10.7 wt % TEGDA (B). Weight ratio QCh:PVA = 2:3, AFS 2.0 kV/cm, total polymer concentration 10 wt %; solvent H_2O/DMSO = 92:8 (w/w).

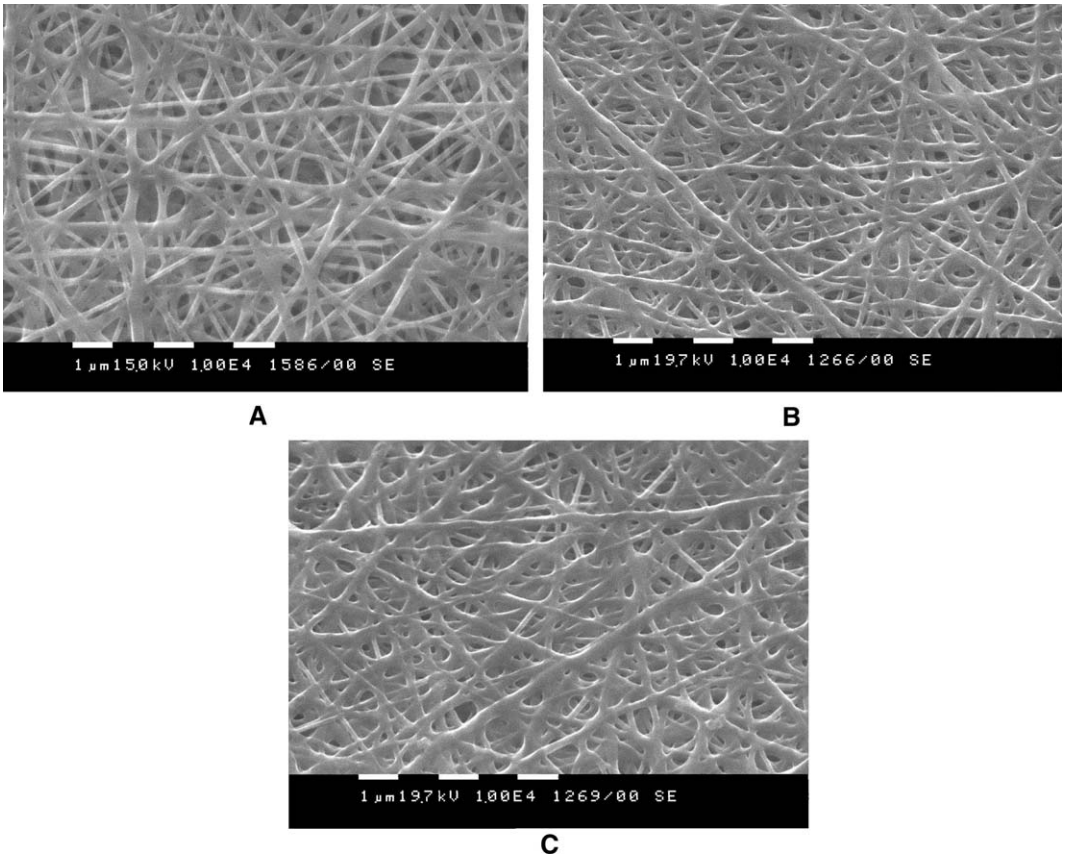

Figure 6. Effect of the water vapour and water on the morphology of the photo-cross-linked QCh/PVA nano-fibres. Non-treated photo-cross-linked mat (A), after contact with water vapour for 1 h (B) and after contact with water for 1 h (C). Weight ratio QCh:PVA = 2:3, total polymer concentration 10 wt % (H_2O/DMSO = 92:8 w/w), AFS 2.0 kV/cm.

environment. In order to retain their unique nano-fibrous structure, photo-mediated cross-linking of electrospun QCh/PVA mats in the solid state was attempted. For this purpose a photo-cross-linking agent, such as triethylene glycol diacrylate (TEGDA), is appropriate. Under UV light-irradiation, TEGDA is able to cross-link both polymers—QCh and PVA, and cross-linking may proceed between chains of one and the same polymer or between the chains of both partners. Appropriate reagents and conditions for photo-mediated cross-linking of the system QCh/PVA were found. Cross-linking of chitosan due to attack of potassium peroxydisulfate on chitosan chains and subsequent recombination has been reported.[30] It cannot be excluded that such a type of cross-linking has also taken place in the case of photo-mediated cross-linking of the nano-fibre QCh/PVA mats. It was found that adding the photoinitiator 2,2-dimethoxy-2-phenylacetophenone (DMPA), ammonium peroxydisulfate and TEGDA as cross-linking agent to the QCh/PVA mixed solution did not impede the electrospinning process and the nano-fibre formation (Fig. 5). The comparison between nano-fibres electrospun in the presence of photo-cross-linking additives and those electrospun without additives showed that the diameters of the nano-fibres decreased on adding cross-linking additives—from 217 to 116 nm (Fig. 5). The size distribution of the cross-linked nano-fibres was narrower. The observed effects might be explained with increase in the conductivity of the solution when the inorganic salt—ammonium peroxydisulfate is added. The conductivity of the solution increased from 2.95 to 4.3 mS/cm when the salt was added. As previously reported, the increase of the charge density and of the conductivity of the solution resulting from the presence of a salt or low-molecular-weight compound with ionisable groups leads to decrease of the diameter of the electrospun fibres and to a smaller number of defects.[15,18,23] Stronger elongation forces are imposed to the jet due to the repulsion of the excess charges, thus resulting in the formation of nano-fibres with smaller diameters.

SEM analyses of the samples indicated that UV irradiation did not cause any change in the fibre morphology. The average diameters of UV-irradiated QCh/PVA nano-fibres, as well as the distributions of their diameters did not differ from that of non-irradiated nano-fibres. It was found that irradiation time necessary for stabilisation of the electrospun QCh/PVA mats against disintegration in water was 10 h. On contact with water or water vapours, a slight increase in the average diameters of the cross-linked QCh/PVA nano-fibres was observed due to swelling and occasional coalescence (Fig. 6). It was found that the photo-cross-linked QCh/PVA nano-fibres swelled in water and the equilibrium swelling degree in water reached 100% (distilled water, 23 °C).

3.3. Antibacterial activity of electrospun photo-cross-linked QCh/PVA mats

The antibacterial activity of quaternary ammonium salts of chitosan is based on the damaging interaction of polycations with negatively charged surface of bacteria resulting in loss of membrane permeability, cell leakage and cell death.[5–7] Quaternised chitosan has shown high antibacterial activity against *S. aureus*.[5] The antibacterial activity of photo-cross-linked electrospun QCh/PVA mats against *S. aureus* and *E .coli* was tested by the viable cell-counting method.[25] *S. aureus* bacteria were killed within 60 min of contact with cross-linked QCh/PVA electrospun mat containing 2845 μg/mL QCh, in contrast to electrospun photo-cross-linked PVA mat, which did not impede the bacteria growth (Fig. 7A). This finding implies that the antibacterial activity of cross-linked electrospun QCh/PVA mats results from quaternised chitosan derivative and that the effect against *S. aureus* is bactericidal rather than bacteriostatic. As seen from the results shown in Figure 7A, both cross-linked electrospun mats and cross-linked QCh/PVA film prepared by solvent casting method with

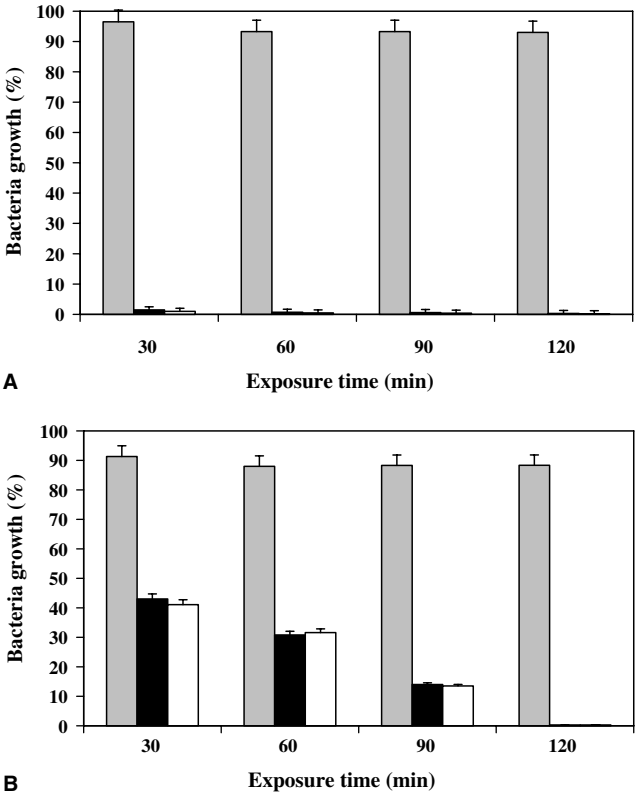

Figure 7. Plot of the bacteria growth, in percent of the control, versus the exposure time: for electrospun cross-linked QCh/PVA mats (□), for cross-linked QCh/PVA films prepared by solvent casting method (■) and for electrospun cross-linked PVA mats (▩). The test was carried out against *S. aureus* (A) and against *E. coli* (B). The error bars are the standard deviations for triplicated experiments.

the same QCh concentration had marked biocide efficiency.

The test showed that MIC of QCh against *E. coli* was 2070 μg/mL. The electrospun QCh/PVA mats were exposed also to Gram-positive bacteria *E. coli*. The reduction of bacteria *E. coli* for photo-cross-linked QCh/PVA nano-fibres containing 2885 μg QCh was 98% after 120 min contact time (Fig. 7B). The antibacterial activity of electrospun QCh/PVA mats is an important property for wound-healing applications because it could contribute to the prevention of secondary infections in wounds by *S. aureus*, resulting in limited scar formation.

4. Conclusions

Quaternised chitosan-containing nano-fibres have been successfully prepared by electrospinning of mixed aqueous solutions of QCh and PVA. The electrospun QCh/PVA fibres had diameters in the 60–200 nm range and narrow diameter distribution. The higher the content of QCh, the smaller was the diameter of the nano-fibres. This was attributed to the increase in solution conductivity on increasing the content of the ionogenic QCh partner. The electrospun QCh/PVA nano-fibrous mats were successfully stabilised against dissolution in aqueous environment using photo-mediated cross-linking. Photo-cross-linked electrospun nano-fibrous QCh/PVA mats had a good bactericidal activity against the Gram-negative bacteria *E. coli* and Gram-positive bacteria *S. aureus*. These characteristic features of the electrospun mats reveal their high potential for wound-dressing applications.

Acknowledgements

Financial support from the Ministry of Education and Science, Bulgarian National Science (Grant NANOBIOMAT, NT-4-01/04) is gratefully acknowledged. The authors thank Dr. N. Starbov (Central Laboratory of Photoprocesses, Bulgarian Academy of Sciences) for conductivity measurement facilities.

References

1. Muzzarelli, R. A. A.; Guerrieri, M.; Goteri, G.; Muzzarelli, C.; Armeni, T.; Ghiselli, R.; Cornelissen, M. *Biomaterials* **2005**, *26*, 5844–5854.
2. Ishihara, M. *TIGG* **2002**, *14*, 331–341.
3. Balakrishnan, B.; Mohanty, M.; Umashankar, P. R.; Jayakrishnana, A. *Biomaterials* **2005**, *26*, 6335–6342.
4. Paul, W.; Sharma, S. P. *Trends Biomat. Art. Organs* **2004**, *18*, 18–23.
5. Kim, C. H.; Choi, J. W.; Chun, H. J.; Choi, K. S. *Polym. Bull.* **1997**, *38*, 387–393.
6. Jia, Z.; Shen, D.; Xu, W. *Carbohydr. Res.* **2001**, *333*, 1–6.
7. Kim, J. Y.; Lee, J. K.; Lee, T. S.; Park, W. H. *Int. J. Biol. Macromol.* **2003**, *32*, 23–27.
8. Kenawy, E.-R.; Layman, J. M.; Watkins, J. R.; Bowlin, G. L.; Matthews, J. A.; Simpson, D. G.; Wnek, G. E. *Biomaterials* **2003**, *24*, 907–913.
9. Li, W.-J.; Laurencin, C. T.; Caterson, E. J.; Tuan, R. S.; Ko, F. K. *J. Biomed. Mater. Res.* **2002**, *60*, 613–621.
10. Kenawy, E. R.; Bowlin, G. L.; Mansfield, K.; Layman, J.; Simpson, D. G.; Sanders, E.; Wnek, G. E. *J. Controlled Release* **2002**, *81*, 57–64.
11. Stitzel, J. D.; Pawlowski, K.; Wnek, G. E.; Simpson, D. G.; Bowlin, G. L. *J. Biomater. Appl.* **2001**, *15*, 1–12.
12. Boland, E. D.; Wnek, G. E.; Simpson, D. G.; Pawlowski, K. J.; Bowlin, G. L. *J. Macromol. Sci., Pure Appl. Chem.* **2001**, *38*, 1231–1243.
13. Deitzel, J.; Kleinmeyer, J.; Hirvonen, J.; Beck Tan, N. *Polymer* **2001**, *42*, 8163–8170.
14. Ding, B.; Kim, H.; Lee, S.; Shao, C.; Lee, D.; Park, S.; Kwag, G.; Choi, K. *J. Polym. Sci., Part B: Polym. Phys.* **2002**, *40*, 1261–1268.
15. Zhang, C.; Yuan, X.; Wu, L.; Han, Y.; Sheng, J. *Eur. Polym. J.* **2005**, *41*, 423–432.
16. Yao, L.; Haas, T. W.; Guiseppi-Elie, A.; Bowlin, G. L.; Simpson, D. G.; Wnek, G. E. *Chem. Mater.* **2003**, *15*, 1860–1864.
17. Zeng, J.; Hou, H.; Wendorff, J. H.; Greiner, A. *Polym. Prepr.* **2003**, *44*, 174–175.
18. Spasova, M.; Manolova, N.; Paneva, D.; Rashkov, I. *e-Polymers* **2004**, *056*, 1–12.
19. Duan, B.; Dong, C.; Yuan, X.; Yao, K. *J. Biomater. Sci., Polym. Ed.* **2004**, *15*, 797–811.
20. Park, W. H.; Jeong, L.; Yoo, D. I.; Hudson, S. *Polymer* **2004**, *45*, 7151–7157.
21. Ohkawa, K.; Cha, D.; Kim, H.; Nishida, A.; Yamamoto, H. *Macromol. Rapid. Commun.* **2004**, *25*, 1600–1605.
22. Li, L.; Hsieh, Y.-L. *Carbohydr. Res.* **2006**, *341*, 374–381.
23. Mincheva, R.; Manolova, N.; Paneva, D.; Rashkov, I. *J. Bioact. Compat. Polym.* **2005**, *20*, 419–435.
24. Shenoy, S. L.; Bates, W. D.; Frisch, H. L.; Wnek, G. E. *Polymer* **2005**, *46*, 3372–3384.
25. Franklin, T. J.; Snow, G. A. *Biochemistry of Antimicrobial Action*; Chapman & Hall: London, 1981; pp 58–60.
26. Koski, A.; Yim, K.; Shivkumar, S. *Mater. Lett.* **2004**, *58*, 493–497.
27. Shenoy, S. L.; Bates, W. D.; Wnek, G. *Polymer* **2005**, *46*, 8990–9004.
28. Fennessey, S. F.; Farris, R. J. *Polymer* **2004**, *45*, 4217–4225.
29. Li, D.; Xia, Y. *Adv. Mater.* **2004**, *16*, 1151–1170.
30. Harish Prashanth, K. V.; Tharanathan, R. N. *Carbohydr. Res.* **2006**, *341*, 169–173.